Vaccine 38 (2020) 5822–5830

Contents lists available at ScienceDirect

Vaccine

journal homepage: www.elsevier.com/locate/vaccine

Influenza hemagglutinin antigenic distance measures capture trends in HAI differences and infection outcomes, but are not suitable predictive tools

Amanda L. Skarlupka [a], Andreas Handel [b], Ted M. Ross [a,c,*]

[a] Center for Vaccines and Immunology, University of Georgia, Athens, GA, USA
[b] Department of Epidemiology and Biostatistics, University of Georgia, Athens, GA, USA
[c] Department of Infectious Diseases, University of Georgia, Athens, GA, USA

ARTICLE INFO

Article history:
Received 30 October 2019
Received in revised form 28 May 2020
Accepted 16 June 2020
Available online 16 July 2020

Keywords:
Antigenic distance
H1 hemagglutinin
Influenza
Sequence
Epitope
Swine
COBRA

ABSTRACT

Vaccination is the most effective method to combat influenza. Vaccine effectiveness is influenced by the antigenic distance between the vaccine strain and the actual circulating virus. Amino acid sequence based methods of quantifying the antigenic distance were designed to predict influenza vaccine effectiveness in humans. The use of these antigenic distance measures has been proposed as an additive method for seasonal vaccine selection. In this report, several antigenic distance measures were evaluated as predictors of hemagglutination inhibition titer differences and clinical outcomes following influenza vaccination or infection in mice or ferrets. The antigenic distance measures described the increasing trend in the change of HAI titer, lung viral titer and percent weight loss in mice and ferrets. However, the variability of outcome variables produced wide prediction intervals for any given antigenic distance value. The amino acid substitution based antigenic distance measures were no better predictors of viral load and weight loss than HAI titer differences, the current predictive measure of immunological correlate of protection for clinical signs after challenge.

1. Introduction

Type A influenza virus (IAV) causes annual, seasonal epidemics and occasionally devastating pandemics [1–3]. Influenza virus infections negatively affect the health of both the human population and the world economy [4–6]. The most effective way to combat influenza is through vaccination. In general, the annual seasonal influenza vaccine is derived of two IAV strains and two influenza B strains (IBV), which represent dominant circulating strains in the human population. However, due to viral evolution and the time manufacturers need to produce the annual vaccine, there is often a mismatch in the antigenic version of the influenza strains selected in the vaccine compared to the influenza viral variants co-circulating during the next influenza season. The effectiveness of the annual vaccine is decreased if the vaccine strain significantly differs from infecting strains [7].

Twice a year (once for each the Northern and Southern hemisphere), governmental agencies recommend to vaccine manufacturers strains to include in the annual vaccine [8]. Influenza experts in epidemiology, public health, and biomedical sciences decide if a change in the vaccine strain is recommended for the upcoming season based upon the most current surveillance, laboratory, and clinical study data at the time. Often, these recommendations are based upon the hemagglutination inhibition (HAI) assay, where the cross reactivity of ferret reference serum produced from infection with influenza vaccine strains is assessed to currently circulating viral variants [9]. An 8-fold drop in HAI activity often results in a strain change recommendation for the next season.

Currently, there is a goal to develop universal influenza vaccines [10]. A variety of strategies are being used that rely on improved antigen development, delivery, adjuvants and immune assays [11,12]. These candidates are assessed for the elicitation of protective immune responses in pre-clinical, and then, clinical studies. To ease the burden of these expensive and time-consuming studies, computational tools have been developed to assist in vaccine selection and to improve vaccine effectiveness [13–16].

The antigenic differences between influenza viruses are defined by the ability of the antibodies to target the surface glycoprotein, the hemagglutinin (HA) and, in particular, the receptor binding site

* Corresponding author at: Center for Vaccines and Immunology, University of Georgia, CVI Room 1504, 501 D.W. Brooks Drive, Athens, GA 30602, USA.
E-mail address: tedross@uga.edu (T.M. Ross).

https://doi.org/10.1016/j.vaccine.2020.06.042
0264-410X/

(RBS) domains on HA [17–19]. The HA amino acid sequence is composed of highly conserved regions that are structurally and functionally necessary to bind to host cell sialic acid receptors and mediate viral fusion and entry to host cells [20]. In addition, there are highly variable head regions of the HA that are primary targets of the host antibody responses [21–23]. These regions, or antigenic sites, differ in size and number on each HA antigen subtype, with the greatest differences observed in HA between subtypes.

Computational methodologies can be used to assist with the vaccine selection process [13–16,24–28]. However, one difficulty is that the genetic similarity between two HA amino acid sequences does not correlate reliably with the antigenic distance between two strains [29]. One or two amino acid differences in the HA can alter the profile of newly elicited antibodies or the ability of previously generated antibodies to neutralize [30–32]. *In vitro* methods have been used to quantify and compare the antigenic distance of different influenza strains using HAI activity by ferret antisera with vaccine efficacy [16,33–37] or with sequence based antigenic distances to correlates of protection [38]. Measuring the HA epitope sequence based antigenic distances between strains in the annual vaccine and circulating strains [39] has been found to correlate with vaccine effectiveness in humans [39-45] or used to predict HAI titers [26]. Analysis of just the immunodominant HA epitopes of the protein sequence and not the entire molecule was proposed to improve the ability to predict HAI titers [35]. The measure of antigenic distance derived from the assumed immunodominant epitope, known as the dominant $p_{epitope}$ value, was validated using historical influenza vaccine effectiveness data from people reporting influenza illness-like symptoms following vaccination with commercial influenza vaccines [39–42,44]. In this study, $p_{epitope}$ and related measures that use protein sequence information to estimate antigenic distance (in the following referred to as antigenic distance measures (ADM)), were examined on whether they could be useful predictors of HAI differences and infection outcomes in animal studies.

2. Materials and methods

2.1. Identities of vaccine, challenge, and HAI panel strains

The strains of influenza used as vaccine antigens, challenge strains, and as an antigen in a hemagglutination inhibition assay are detailed in Table 1. The accession numbers, or appropriate reference, for the HA amino acid sequences used for the antigenic distance calculations are included (Suppl. Table 1). Strains included H1 influenza from both human and swine origin as indicated.

2.2. Mouse vaccinations and infections

Mouse immunological and virological data were obtained from previous studies [46,47]. Briefly, BALB/c mice (Mus musculus, female, 6–8 weeks old) were purchased from Envigo (Indianapolis, IN, USA) and housed in microisolator units. Animals were allowed free access to food and water and cared for under USDA guidelines for laboratory animals. All procedures were reviewed and approved by the University of Georgia Institutional Animal Care and Use Committee (IACUC) #2016-02-011-Y3-A7. Mice were randomly divided into 10 groups (n = 11/group) and were vaccinated with virus-like particles (VLPs) expressing H1 hemagglutinins (HA) of human, swine or COBRA origin. The corresponding HA and a wild-type mismatched influenza neuraminidase (A(H7N3)/mallard/Alberta/24/2001) were pseudotyped onto an HIV GAG protein to generate a VLP. Mice were vaccinated with each VLP plus an MF59-like squalene oil-in-water adjuvant at day 0 and 28. A mock vaccinated group was included which received a phosphate-buffered saline (PBS) and adjuvant vaccination. Serum samples were collected at days 42 and 54 post-vaccination. Vaccinated mouse sera were tested for HAI activity against a panel of H1 viruses (Table 1).

Vaccinated mice were challenged with 5×10^4 plaque forming unit (PFU) (10X 50% lethal doses [LD_{50}]) wild-type A(H1N1)/California/07/2009 or 1×10^7 PFU A(H1N2)/swine/North Carolina/152702/2015 in a volume of 50 µl. Mice were monitored daily for 14 days for weight loss, disease signs and death. Mice from each group (n = 3) were euthanized on day 3 post-infection for lung harvest. Lung tissue was snap frozen on dry ice, and stored at −80 °C for future viral titration. Mice were humanly euthanized when they reached the humane endpoint of 20% original body weight loss or a cumulative clinical disease score of 3 (lethargy = 1, hunched posture = 1, rough fur = 1, weight loss 15%-20%=1, weight loss >20% of original body weight = 3). All procedures were performed in accordance with the Guide for the Care and Use of Laboratory Animals [48], Animal Welfare Act [49], and Biosafety in Microbiological and Biomedical Laboratories [50] .

2.3. Ferret infections

Immunological data of ferrets preimmunized to A(H1N1)/California/07/2009, A(H1N1)/Brisbane/59/2007, or A(H1N1)/Singapore/6/1986 were obtained from previous publication [51]. Briefly, fitch ferrets (*Mustela putorius furo*, female, 6 to 12 months of age, de-scented) were purchased from Triple F Farms (Sayre, PA). Ferrets were pair housed in stainless steel cages (Shor-line, Kansas City, KS) containing Sani-Chips laboratory animal bedding (P.J. Murphy Forest Products, Montville, NJ). Ferrets were provided with Teklad Global Ferret Diet (Harlan Teklad, Madison, WI) and fresh water ad libitum. The University of Georgia Institutional Animal Care and Use Committee approved all experiments, which were conducted in accordance with the National Research Council's *Guide for the Care and Use of Laboratory Animals*, The Animal Welfare Act, and the CDC/NIH's *Biosafety in Microbiological and Biomedical Laboratories* guide. Ferrets (n = 4) were infected with

Table 1
HAs used as HAI antigens, vaccine components, and viral challenge strains.

HAI Antigen		Vaccine and HAI Antigen		
Swine Isolate	Human Isolate	Swine Isolate	Human Isolate	COBRA
A/Swine/IA/1973	A/SC/1/1918	A/Swine/WI/125/1997	A/Chile/1/1983	SW1
A/Swine/NC/93523/2001	A/Weiss/1/1943	A/Swine/IN/P12439/2000	A/Singapore/6/1986	SW2
A/Swine/NC/A01377454/2014	A/Fort Monmouth/1/1947	A/Swine/Spain/50047/2003	A/New Caledonia/20/1999	SW3
A/Swine/NE/A01444614/2013	A/Denver/1/1957	A/Swine/Korea/Asan04/2006	A/Brisbane/59/2007	SW4
A/Swine/MO/A01203163/2012	A/NJ/11/1976	A/Swine/Zhejiang/1/2007		X-3
A/Swine/OK/A0149501/2011	A/USSR/90/1977	A/Swine/NC/02744/2009		X-6
A/Swine/NC/5043-1/2009	A/Brazil/11/1978	A/Swine/NC/34543/2009		P-1
A/Swine/CO/SG1322/2009	A/TX/36/1991	A/Swine/MN/A01489606/2015		
A/Swine/OH/511445/2007	A/Beijing/262/1995	Vaccine, HAI Antigen, and Challenge Strain		
	A/Solomon Islands/3/2006	A/Swine/NC/152702/2015	A/CA/07/2009	

one of the three H1N1 influenza viruses (10^6 PFU/ 1 ml) intranasally. Animals were monitored daily during the infection for adverse events, including weight loss, loss of activity, nasal discharge, sneezing, and diarrhea and allowed to recover. All blood was harvested from anesthetized ferrets via the anterior vena cava at day 14 post-infection. Blood was transferred to a centrifuge tube and centrifuged at 6000 rpm. Clarified serum was collected, frozen at −20 ± 5 °C and used for HAI assays.

2.4. Hemagglutination inhibition (HAI) assay

The hemagglutination inhibition (HAI) assay was used to assess functional antibodies specific to the receptor binding site of the HA that inhibit the agglutination of turkey erythrocytes. The protocols were adapted from the WHO laboratory influenza surveillance manual [52] and were performed as previously described [53]. Briefly, to inactivate nonspecific inhibitors, sera were treated with receptor-destroying enzyme (RDE) (*Denka Seiken*, Co., Japan) prior to being tested. Three-parts RDE were added to one-part sera and incubated overnight at 37 °C. Following RDE inactivation by incubation at 56 °C for 30 min, six-parts phosphate-buffered saline pH 7.2 (PBS, Gibco) were added. RDE-treated sera were diluted in a series of two-fold dilutions in V-bottom microtiter plates. An equal volume of virus or virus-like particle, adjusted to approximately 8 hemagglutination units (HAU)/50 µl, was added to each well. The plates were agitated, covered, and incubated at room temperature (RT) for 20 min. Then, 0.8% of turkey red blood cells (RBCs; *Lampire Biologicals*, Pipersville, PA, USA) in PBS were added. All RBCs were stored at 4 °C and used within 72 h of preparation. The plates were agitated and covered. The RBCs were allowed to settle for 30 min at RT. The HAI titer was determined by the reciprocal dilution of the last well that contained agglutinated RBCs. Positive and negative serum controls were included for each plate. All mice and ferrets were negative (HAI < 1:10) for preexisting antibodies to currently circulating human influenza viruses prior to vaccination or challenge and seroprotection was defined as HAI titer ≥ 1:40 and seroconversion as a 4-fold increase in titer compared to baseline, as per the WHO and European Committee for Medicinal Products to evaluate influenza vaccines [54]. The limit of detection for $\log_2$ HAI titer was 3.32. If below the limit of detection, 2.32 $\log_2$ HAI titer was used for mathematical calculations.

2.5. Viral lung titers

Plaque assay was performed according to previously described protocols [55]. In brief, lungs were homogenized in 1 ml Dulbecco's Modified Eagle Medium (DMEM), and the supernatant was collected by spinning the homogenized samples at 2000 rpm for 5 min. Low passage (<30) Madin-Darby Canine Kidney (MDCK) cells were plated at a confluency of 1×10^6 cell per well of a six-well plate (*Greiner bio-one*, NC, USA) one day before the assay. MDCK cells were infected with different dilutions of samples in 100 µl of DMEM supplemented with penicillin-streptomycin. After 1 h incubation at RT, the medium was removed, and cells were washed twice with fresh DMEM. After the addition of 2 ml of Modified Eagle Medium (MEM) medium at 2 µg/mL TPCK-trypsin and 0.8% agarose (*Cambrex*, East Rutherford, NJ, USA), cells were incubated for 72 h at 37 °C with 5% CO_2. Agarose was removed, and the cells were fixed with 10% buffered formalin and stained with 1% crystal violet (*Fisher Science Education*) for 15 min. The crystal violet was removed by rinsing thoroughly in distilled water. The numbers of plaques were counted in duplicate. Duplicates were then averaged and transformed by $\log_{10}$. The virus titer was analyzed as the average $\log_{10}$ PFU/lung for each individual mouse.

2.6. Amino acid based antigenic distance measure (ADM) calculation

The five antigenic sites used in the calculation of the H1 HA subtype antigenic distance were outlined previously [41]. Due to the inclusion of the pandemic HAs, the A(H1N1)/California/04/2009 numbering scheme was used with a maximum length of 549 residues for the HA0 [41]. The amino acid numbering begins following the seventeen amino acids in the signal peptide [56-58]. The HA1 region was defined as amino acids 1–327. The antigenic sites include the amino acids predicted to be important to vaccine efficacy: neutralizing-antibody binding residues, structure/sequence homologues of known H3 epitopes, and protein surface residues with high information entropy (Table 2) [41]. The following equations were used to calculate the antigenic distances:

$$p_{sequence} = \frac{number\ of\ substitutions\ in\ entire\ HA\ sequence}{total\ number\ of\ amino\ acids\ in\ entire\ HA\ sequence}$$

$$p_{HA1} = \frac{number\ of\ substitutions\ in\ HA1}{total\ number\ of\ amino\ acids\ in\ HA1}$$

$$p_{all-epitope} = \frac{number\ of\ substitutions\ in\ all\ epitopes}{total\ number\ of\ amino\ acids\ in\ all\ epitopes}$$

$$p_{epitopex} = \frac{number\ of\ substitutions\ in\ epitope\ x}{total\ number\ of\ amino\ acids\ in\ epitope\ x}$$

$$p_{epitope} = max p_{epitopex}$$

ADM were determined through protein alignment. Briefly, the HA0 was aligned utilizing Geneious alignment with global alignment with free end gaps and a cost matrix Blosum62 with open gap penalty 12, and gap extension penalty 3, with refinement iterations of 2 (Geneious v11.1.5). The HA1 portions (1-327AA) were extracted from the alignment. From which, all or individual antigenic sites were extracted and the differing number of amino acids between two viral strains were determined.

2.7. HAI titer difference calculation

The original raw HAI data were in two-fold serial dilution titers and transformed by $\log_2$. From those transformed values, the mean $\log_2$ HAI titer was calculated for each vaccine:challenge virus combination. Outliers were not removed, but mock controls (PBS vaccinated) were removed from analysis. The difference between reference HAI titer and HAI titer for a specific strain was computed as $\Delta HAI = \log_2(HAI_{ref}) - \log_2(HAI_s)$.

2.8. Regression analysis between ADM and correlates of protection

Linear regression models, as done previously with antigenic measures [59], were fit to the data with the different antigenic

Table 2
Amino acid residues used to calculate the ADM of vaccine and challenge virus combinations.

Antigenic Site	Amino Acid Residue
A (Sa)	118, 120, 121, 122, 126,-129 1, 132-135, 137, 139-143, 146, 147, 149, 165, 252, 253
B (Sb)	124, 125, 152-157, 160, 162, 183-187 189-191, 193-196
C	34-38, 40, 41, 43-45, 269-274, 276-278, 283, 288, 292, 295, 297, 298, 302, 303, 305-310,
D (Ca)	89, 94-96, 113, 117, 163, 164, 166174, 176-178, 200, 202, 204-216, 222-227, 235, 237, 241, 243-245
E (Cb)	47, 48, 50, 51, 53, 54, 56-58, 66, 68-75 78-80, 82-86, 102, 257-261, 263, 267

measures as predictors, and HAI differences, lung titer and percent weight loss as outcomes. The adjusted R^2 was reported for all linear fits. The 95% confidence and prediction intervals were computed for each model with R version 3.6.2 using RStudio version 1.2.5033 [60]. The day 6 percent weight loss for mice was determined by dividing weight on day six post-challenge by the original day 0 weight and which was expressed as a percentage. Further analysis including the data below the limit of detection were analyzed separately.

3. Results

3.1. ADM describe the trend of ΔHAI titer of H1 influenza viruses in mice

The goal of this study was to determine if the ADM determined from influenza HA amino acid sequences may be a predictive measure for HA-induced HAI activity in collected antisera. These values, $p_{sequence}$, p_{HA1}, $p_{all\text{-}epitope}$, and $p_{epitope}$, are different attempts to measure the antigenic distance between two different viruses [29].

Three hundred and sixteen ΔHAI titers from vaccinated mice were examined for the linear relationship between the ΔHAI titers and ADM. The ADM had ranges starting at 0.0 with varying maximums ($p_{sequence}$ = 0.222, p_{HA1} = 0.303, $p_{all\text{-}epitope}$ = 0.528, $p_{epitope}$ = 0.864). There was a linearly increasing trend of HAI titer difference as antigenic distance increased ($p < 0.0001$) (Fig. 1; Suppl. Fig. 1). The adjusted R^2 increased as the antigenic measure became more specific ($p_{sequence} < p_{HA1} < p_{all\text{-}epitope} < p_{epitope}$). Thus, $p_{epitope}$ was the best among the ADM in describing ΔHAI. Nevertheless, the R^2 values were all low, with a maximum value of 0.288 for the $p_{epitope}$ antigenic distance (Table 3; Suppl. Table 1). The variability of HAI differences for any value of antigenic distance was wide and ranged from a minimum of 0.868 ΔHAI at a $p_{epitope}$ of 0.545 and a maximum of 12.5 ΔHAI at a value of 0.864 ADM, with a mean variability of 5.60 ΔHAI.

3.2. ADM are poor predictors of ΔHAI titer of H1 influenza viruses in mice

To evaluate the ability of the ADM to predict ΔHAI, the 95% prediction intervals were computed. Those intervals are wide; the mean $p_{epitope}$, 0.420 units, has the narrowest prediction interval of the data. The predictive interval for the mean, around the fitted estimate of 4.056 ΔHAI was ±4.816 ΔHAI. The predictive intervals are wider than this range for any other given antigenic distance value. With widths greater than ±2.0 ΔHAI, the measures were not suitable as predictive tools for outcomes of HAI assays.

3.3. $P_{epitope}$ shows improved, but still limited, performance for COBRA vaccines

To evaluate if ADM might perform better for a specific type of vaccine, namely the COBRA vaccines [46,51], another analysis was performed on a subset of the data. Only mice vaccinated with

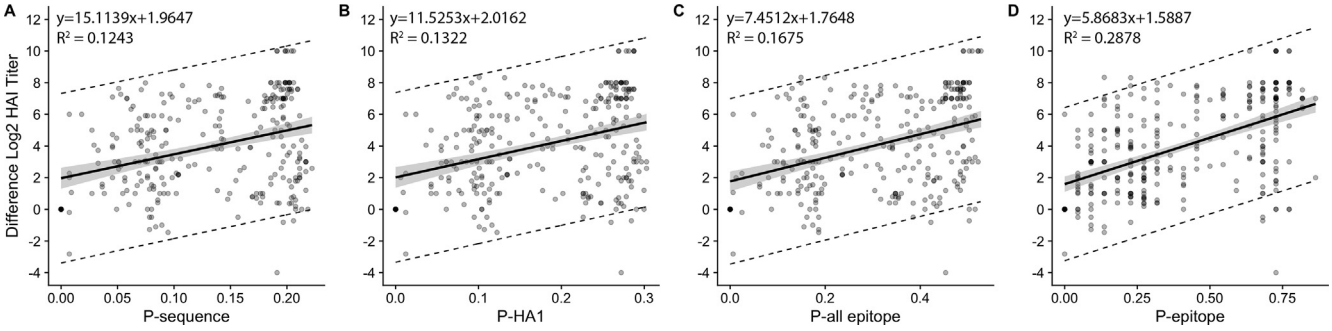

Fig. 1. Amino acid sequence based antigenic distances modeled against the change in HAI titer of H1 influenza in the mouse model. Linear regression of $p_{sequence}$ (A), p_{HA1} (B), $p_{all\text{-}epitope}$ (C), and $p_{epitope}$ antigenic distances (D) against the ΔHAI titers to homologous control elicited in BALB/C mice. The 95% confidence intervals are depicted with grey shading. The 95% prediction intervals are depicted by dashed lines.

Table 3
Summary of resultant equations from best-fit analysis.

Dependent variable	Independent Variable	Equation	d.f.	t-Value	P-Value	Adjusted R^2
Mouse ΔHAI	$P_{sequence}$	$y = 15.1139x + 1.9647$	291	6.515	<0.0001	0.1243
	P_{HA1}	$y = 11.5253x + 2.0162$	301	6.856	<0.0001	0.1322
	$P_{all\text{-}epitope}$	$y = 7.4514x + 1.7648$	306	7.924	<0.0001	0.1675
	$P_{epitope}$	$y = 5.8683x + 1.5887$	314	11.328	<0.0001	0.2878
Ferret ΔHAI	$P_{sequence}$	$y = 32.7805x + 1.5102$	28	4.539	<0.0001	0.4034
	P_{HA1}	$y = 24.1281x + 1.4296$	28	4.648	<0.0001	0.5153
	$P_{all\text{-}epitope}$	$y = 12.8958x + 1.4243$	28	4.579	<0.0001	0.4078
	$P_{epitope}$	$y = 8.9706x + 0.9403$	28	5.616	<0.0001	0.5129
Mouse Day 3 Viral Lung Titer	$P_{sequence}$	$y = 9.1448x + 2.7541$	21	1.671	0.10960	0.0753
	P_{HA1}	$y = 7.3363x + 2.6468$	21	1.892	0.07232	0.105
	$P_{all\text{-}epitope}$	$y = 4.586x + 2.552$	21	2.189	0.040025	0.147
	$P_{epitope}$	$y = 5.0661x + 2.1251$	22	5.543	<0.0001	0.5638
	ΔHAI	$y = 0.41453x + 1.73092$	22	4.285	0.0003	0.4302
Mouse Day 6 Weight Loss	$P_{sequence}$	$y = 32.410x + 7.936$	21	1.556	0.13462	0.06069
	P_{HA1}	$y = 7.3363x + 2.6468$	21	1.763	0.09248	0.08742
	$P_{all\text{-}epitope}$	$y = 16.153x + 7.247$	21	2.013	0.05715	0.1218
	$P_{epitope}$	$y = 17.587x + 5.561$	22	4.816	<0.0001	0.491
	ΔHAI	$y = 1.4931x + 3.9187$	22	4.085	0.0005	0.4054

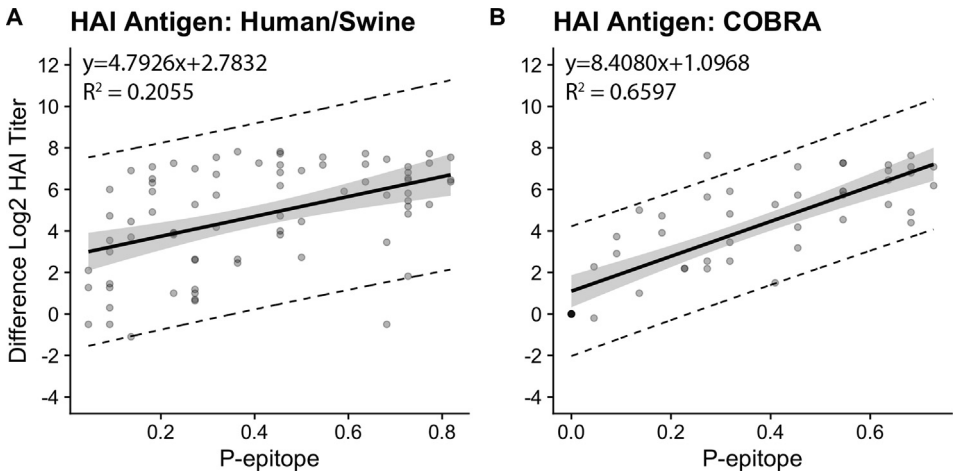

Fig. 2. The $p_{epitope}$ antigenic distance better describes computationally designed interactions, than wild-type HAI antigen interactions. Linear regression of $p_{epitope}$ antigenic distance against the ΔHAI titers to homologous control elicited in BALB/C mice. The vaccine antigen for all datapoints was a COBRA HA antigen. The HAI antigen was either of wild-type origin (A) or a COBRA VLP (B). The 95% confidence intervals are depicted with grey shading. The 95% prediction intervals are depicted by dashed lines.

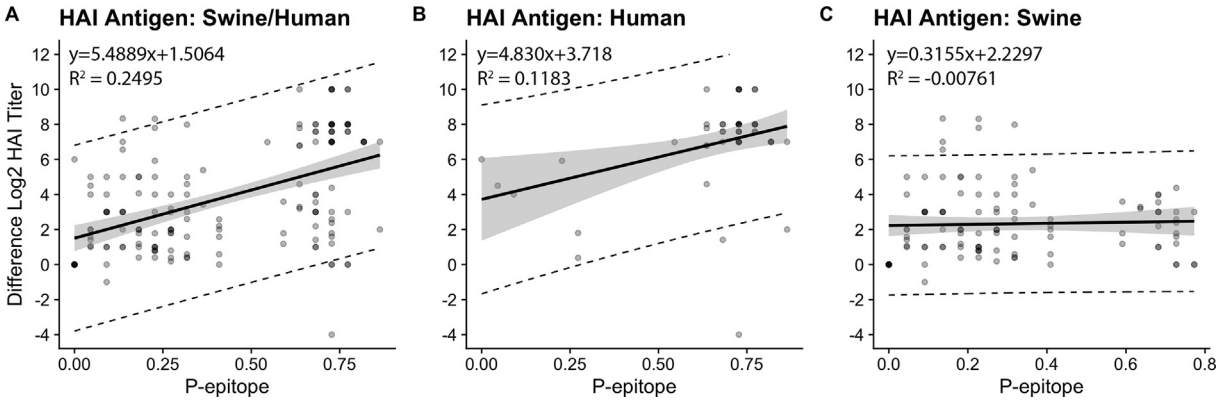

Fig. 3. The interactions of swine origin HA antigens with HAI antigens are not a function of the $p_{epitope}$ antigenic distance. Linear regression of $p_{epitope}$ antigenic distance against the ΔHAI titers to homologous control elicited in BALB/C mice. The vaccine antigen for all datapoints was a swine origin HA antigen. The HAI antigen was both human and swine (A), only human (B), or only swine (C) origin. The 95% confidence intervals are depicted with grey shading. The 95% prediction intervals are depicted by dashed lines.

a COBRA vaccine were analyzed. The $p_{epitope}$ ADM was focused on since it performed best in the previous analyses. The prediction intervals for COBRA vaccinated mice tested against a wild-type human or swine H1 influenza strain were still wide, with a minimum spread of ±4.479 ΔHAI around the fitted value of 4.724 ΔHAI at the mean $p_{epitope}$ ADM of 0.405 units (Fig. 2A). However, the COBRA vaccinated mouse sera tested against COBRA VLPs in the HAI assay had smaller prediction intervals than most other combinations of ±3.06 ΔHAI around the fitted value of 4.154 ΔHAI at the mean $p_{epitope}$ of 0.364 (Fig. 2B). The same subset was evaluated with the inclusion of the points below the limit of detection and a similar trend was observed (Suppl. Fig. 2; Suppl. Table 2).

3.4. $P_{epitope}$ poorly describes ΔHAI for swine H1 influenza viruses in mice

One of the most novel aspects of this dataset was the inclusion of the swine origin influenza as HAI antigens and as vaccine antigens. When the swine antisera were matched with only human and swine wild-type HAI antigens (removal of COBRA HAI antigens), there was again an increasing trend between ADM and ΔHAI (Fig. 3A). However, upon subsetting the HAI antigen by host origin, the swine anti-sera were less HAI cross-reactive with the human antigens (Fig. 3B), with most of the datapoints having a large $p_{epitope}$ and a large ΔHAI titer. Interestingly, an analysis of swine antisera against different swine viruses did not show a correlation (R^2 = −0.00761) between $p_{epitope}$ and ΔHAI (Fig. 3C). The same subset was evaluated with the inclusion of the points below the limit of detection and a similar trend was also observed (Suppl. Fig. 3; Suppl. Table 2).

3.5. ADM describe the trend of ΔHAI titer of H1 influenza viruses in ferrets

To determine if the trend observed in the mouse model was consistent across animal models or an artifact of the mouse model, the ΔHAI titer of antisera collected from ferrets infected with influenza virus was used for analysis. Thirty different antisera:HAI antigen combinations from challenged ferrets were examined for the linear relationship between the ΔHAI titers and ADM. The measures all had a range starting at 0.0 with varying maximums ($p_{sequence}$ = 0.199, p_{HA1} = 0.275, $p_{all\text{-}epitope}$ = 0.522, $p_{epitope}$ = 0.727). There was a linearly increasing trend of HAI titer difference as antigenic distance increased ($p < 0.0001$) (Fig. 4). The adjusted R^2 remained similar across the four ADM; there was no increasing trend, as seen with the mouse model. The ADM were higher than

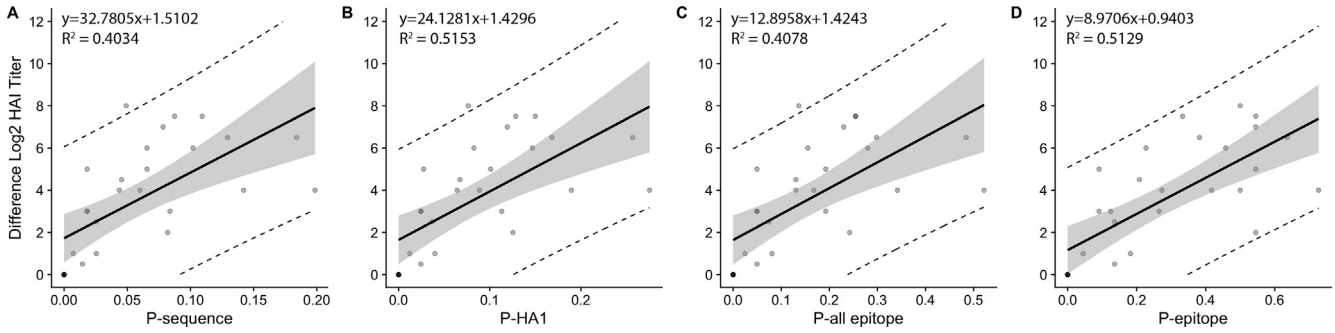

Fig. 4. Amino acid sequence based antigenic distances modeled against the change in HAI titer for human H1N1 subtype HAI data in the ferret model. Linear regression of $p_{sequence}$ (A), p_{HA1} (B), $p_{all\text{-}epitope}$ (C), and $p_{epitope}$ antigenic distances (D) against the ΔHAI titers to homologous control elicited in pre-immune ferrets. The 95% confidence intervals are depicted with grey shading. The 95% prediction intervals are depicted by dashed lines.

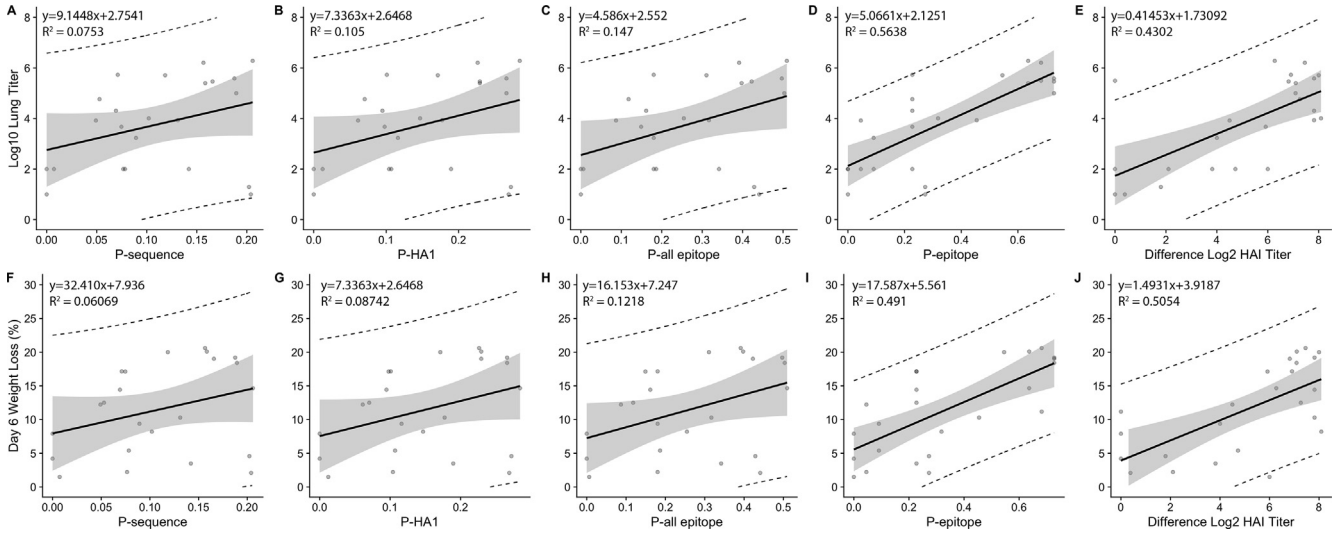

Fig. 5. The use of *in vivo* challenge data from the mouse model for linear regression with different antigenic distances. The sequence based and HAI based antigenic distances were linearly modeled with the mean $\log_{10}$ lung viral titers (A–E) and day 6 percent weight loss (F–J) in mice after infection with either a human H1N1 (CA/09) or swH1N2 virus (SW/NC/15). The 95% confidence intervals are depicted with grey shading. The 95% prediction intervals are depicted by dashed lines.

the mouse model, with a maximum value of 0.515 for the p_{HA1} antigenic distance (Table 3), likely in part due to less data available for these analyses. There was, again, a wide spread in ΔHAI for any value of antigenic distance with a mean variance of 4.78 ΔHAI for the $p_{epitope}$ ADM. The same dataset was evaluated with the inclusion of the points below the limit of detection and a similar trend was observed (Suppl. Fig. 4; Suppl. Table 2).

This suggests that similar to the mouse results, the ADM can capture the overall trend in ΔHAI but it is not possible to use them to predict outcomes of an HAI assay with much precision.

3.6. ADM and ΔHAI show similar correlations with viral load and weight loss following infection in mice

In a last set of analyses, ADM or ΔHAI were assessed to determine if either correlated with two important infection outcomes, namely the peak viral lung titer and weight loss in mice. In total, there were twenty-four or twenty-three vaccine and challenge pairs analyzed depending on predictor variable (Table 3). Among the ADM, $p_{all\text{-}epitope}$, and $p_{epitope}$, showed statistically significant correlations with lung virus titer, so did ΔHAI (Fig. 5A–E; Table 3). The $p_{all\text{-}epitope}$ had a smaller R^2 value of 0.147 compared to the other measures, such as 0.569 for $p_{epitope}$ and 0.430 for ΔHAI titer. The $p_{epitope}$ had the narrowest prediction intervals at the mean value of 0.337 ADM, for a fitted value of 3.833 +/- 2.3144 $\log_{10}$ lung titer.

The challenged mouse day 6 weight dataset revealed that of the ADM only the $p_{epitope}$ and ΔHAI titer were significant (Fig. 5F–J). The R^2 for these two measures were 0.491 and 0.405, respectively. Hence, the variation in weight loss in mice was better explained by the $p_{epitope}$ than the other antigenic measures. For all predictor and outcome variables in this analysis, prediction intervals were wide with the narrowest prediction intervals for the dataset at the $p_{epitope}$ mean of 0.337 units with a fitted weight loss of 11.490 +/- 9.87% (Fig. 5), thus suggesting that while both $p_{epitope}$ and ΔHAI can capture the overall trend, in lung titer and weight loss, neither quantity is useful for precise predictions.

4. Discussion

In this study, datasets from previous influenza virus vaccination and infection studies [46,51] were used to determine the relationship between several ADM and HAI titer differences, viral lung titer, and weight loss. The ADM correlated with the difference in HAI titer but resulted in large prediction intervals (Figs. 1–3). The relationships of ADM and ΔHAI were similar in the ferret and mouse models (Figs. 1 and 4; Table 3). When comparing the ADM to viral lung titer and percent weight loss, only the $p_{epitope}$

and ΔHAI adequately described the overall trends. The use of ADM as a predictive measure of ΔHAI titer, viral lung titer, and weight loss was determined not to be applicable due to wide predictive intervals for each outcome.

Previous studies compared HA-based computational ADM to ferret antisera HAI-based antigenic distances as predictors of inactivated influenza vaccine efficacy in humans and found that the computational ADMs correlated better with vaccine efficacy than HAI-based measures did [39-42,44]. This study differed from the previous studies in that the outcome of interest was ΔHAI titer and murine clinical signs rather than influenza-like symptoms in vaccinated persons. Unlike in the human system used for the previous studies, the mice were not pre-immune to influenza. Although the mice were exposed to influenza HA through three vaccinations, the immune responses to infection and vaccination are not equivalent [61,62]. The mechanism of exposure contributes to the epitope immunodominance of the antigen [63,64]. Both vaccination and infection induce a systemic antibody response. Yet the live influenza infection leads to local immune and cytotoxic T-cell responses which could be captured in the original studies that used humans with pre-existing immunity and an outcome of influenza-like illness through T-cell epitope similarity potentially having some multicollinearity with B-cell epitope similarity through the genetic distance of the two genomes being compared [62,65]. Furthermore, the ADMs may correlate better with vaccine efficacy in a pre-immune human model where immunodominance drives the antibody response to the measured dominant $p_{epitope}$. In a naïve vaccinated model, the antigen immunodominance could be directed to a different site thus not being captured by the ADM and contributing to the large variances of HAI titers observed at any given ADM, but further analysis would need to be conducted to confirm. In addition, the wide variability of HAI titers across ADM may have been influenced by including viruses isolated from different animal species [66,67]. A host origin different from human may have species-specific epitope signatures that lead to uncommon antigenic regions not included in the definition of the antigenic regions since they are not shared across all species [35,68-71].

Considering all of these confounding factors, equating the immunodominant site to the most variable region, as used in this and previous analyses [41], may be inappropriate and may have contributed to the low correlation between the ADM and ΔHAI titers in an analysis with such variety of viral origins and animal models. The determination of these origin and species-specific antibody binding and immunodominance characteristics require future in depth studies on host antibody kinetics and viral escape mutant analysis. Inferences from antibody responses from animal data and the correlations between amino acid sequences, HAI titers, and viral protection should be cautiously made.

Furthermore, strains may contain variations in their antigenic and neutralizing sites in undefined locations on the HA protein or on another component contributing to the observed poor correlation [72,73]. Other methods may be proposed over the purely amino acid sequence based methods such as including limited antisera data and genetic variation to achieve a finer resolution as previous shown with H3N2 [74]. Other correlates of protection, such as total antibody binding or neutralization titers, which have been shown to be more reliable than HAI, could be investigated to determine if they correlate better with the ADM [75,76]. The protective contribution of T-cell epitopes should be considered in pre-immune models especially due to human's pre-existing immunity [77].

The ability to accurately and precisely quantify antigenic distance at the amino acid sequence level would be a valuable tool for influenza virus research. Currently, the phylogenetic distance between a pair of viral gene segments is not an accurate predictor of antigenic distance [72]. Therefore, *in-silico* methods for the antigenic characterization of influenza viruses are being developed and improved [27]. However, here we report that the ADM analyzed do not provide a method useful for predicting the ΔHAI response from a variety of influenza host origins and vaccine and challenge strain combinations, and the method did not correlate any better than ΔHAI titers in determining viral challenge outcomes. With the potentially additive confounding factors of the species of the virus and antibody origin, as well as, antigen delivery affecting the definition of antigenic regions. Hence, this antigenic distance measure needs to be further optimized before use in animal model based vaccine research and development.

Author contributions

ALS conceptualized and wrote the manuscript, designed, and performed experiments and analyzed data; AH conceptualized and supervised the analysis and edited the manuscript; TMR acquired funding, helped to conceptualize and edited the manuscript.

Declaration of Competing Interest

The authors declare that they have no known competing financial interests or personal relationships that could have appeared to influence the work reported in this paper.

Acknowledgments

The authors would like to thank Donald Carter for animal technical assistance and Dr. Mark Tompkin's laboratory for graciously providing the A/Swine/North Carolina/152702/2015 virus and HA amino acid sequence data. We would also like to thank Dr. Deborah A. Keys, Israel Rivera, Steven B. Hancock, and Z. Beau Reneer for helpful discussions and comments. The following reagents were obtained through the NIH Biodefense and Emerging Infections Research Resources Repository, NIAID, NIH: Georgia Research Alliance as an Eminent Scholar. This work was funded, in part, by the U.S. NIH/NIAID Collaborative Influenza Vaccine Innovation Centers (CIVICs) contract 75N93019C00052 by the University of Georgia (UGA) (UGA-001). In addition, TMR is supported by the Georgia Research Alliance as an Eminent Scholar.

Appendix A. Supplementary material

Supplementary data to this article can be found online at https://doi.org/10.1016/j.vaccine.2020.06.042.

References

[1] Fedson DS. Influenza, evolution, and the next pandemic. Evol Med Public Health 2018;2018:260–9.
[2] Reneer ZB, Ross TM. H2 influenza viruses: designing vaccines against future H2 pandemics. Biochem Soc Trans 2019;47:251–64.
[3] Cox NJ, Subbarao K. Global epidemiology of influenza: past and present. Annu Rev Med 2000;51:407–21.
[4] Sellers SA, Hagan RS, Hayden FG, Fischer 2nd WA. The hidden burden of influenza: A review of the extra-pulmonary complications of influenza infection. Influenza Other Respir Viruses 2017;11:372–93.
[5] Putri W, Muscatello DJ, Stockwell MS, Newall AT. Economic burden of seasonal influenza in the United States. Vaccine 2018;36:3960–6.
[6] McElwain TF, Thumbi SM. Animal pathogens and their impact on animal health, the economy, food security, food safety and public health. Rev Sci Tech 2017;36:423–33.
[7] Tricco AC, Chit A, Soobiah C, Hallett D, Meier G, Chen MH, et al. Comparing influenza vaccine efficacy against mismatched and matched strains: a systematic review and meta-analysis. BMC Med 2013;11:153.

[8] Grohskopf LA, Alyanak E, Broder KR, Walter EB, Fry AM, Jernigan DB. Prevention and Control of Seasonal Influenza with Vaccines: Recommendations of the Advisory Committee on Immunization Practices - United States, 2019–20 Influenza Season. MMWR Recomm Rep 2019;68:1–21.
[9] Organization WH. Recommended composition of influenza virus vaccines for use in the 2019-2020 northern hemisphere influenza season; 2019.
[10] Paules CI, Fauci AS. Influenza Vaccines: Good, but We Can Do Better. J Infect Dis. 2019;219:S1–4.
[11] Yakubogullari N, Genc R, Coven F, Nalbantsoy A, Bedir E. Development of adjuvant nanocarrier systems for seasonal influenza A (H3N2) vaccine based on Astragaloside VII and gum tragacanth (APS). Vaccine. 2019;37:3638–45.
[12] Vemula SV, Sayedahmed EE, Sambhara S, Mittal SK. Vaccine approaches conferring cross-protection against influenza viruses. Expert Review of Vaccines. 2017;16:1141–54.
[13] Morris DH, Gostic KM, Pompei S, Bedford T, Luksza M, Neher RA, et al. Predictive modeling of influenza shows the promise of applied evolutionary biology. Trends Microbiol 2018;26:102–18.
[14] Luksza M, Lassig M. A predictive fitness model for influenza. Nature 2014;507:57–61.
[15] Neher RA, Russell CA, Shraiman BI. Predicting evolution from the shape of genealogical trees. Elife. 2014; 3.
[16] Bedford T, Suchard MA, Lemey P, Dudas G, Gregory V, Hay AJ, et al. Integrating influenza antigenic dynamics with molecular evolution. Elife 2014;3:e01914.
[17] Liu M, Zhao X, Hua S, Du X, Peng Y, Li X, et al. Antigenic Patterns and Evolution of the Human Influenza A (H1N1) Virus. Sci Rep. 2015;5:14171.
[18] Cattoli G, Milani A, Temperton N, Zecchin B, Buratin A, Molesti E, et al. Antigenic drift in H5N1 avian influenza virus in poultry is driven by mutations in major antigenic sites of the hemagglutinin molecule analogous to those for human influenza virus. J Virol 2011;85:8718–24.
[19] Ndifon W, Wingreen NS, Levin SA. Differential neutralization efficiency of hemagglutinin epitopes, antibody interference, and the design of influenza vaccines. Proc Natl Acad Sci U S A. 2009;106:8701–6.
[20] Xiong X, McCauley JW, Steinhauer DA. Receptor binding properties of the influenza virus hemagglutinin as a determinant of host range. Curr Top Microbiol Immunol. 2014;385:63–91.
[21] Caton AJ, Brownlee GG, Yewdell JW, Gerhard W. The antigenic structure of the influenza virus A/PR/8/34 hemagglutinin (H1 subtype). Cell 1982;31:417–27.
[22] Tsuchiya E, Sugawara K, Hongo S, Matsuzaki Y, Muraki Y, Li ZN, et al. Antigenic structure of the haemagglutinin of human influenza A/H2N2 virus. J Gen Virol. 2001;82:2475–84.
[23] Webster RG, Laver WG. Determination of the number of nonoverlapping antigenic areas on Hong Kong (H3N2) influenza virus hemagglutinin with monoclonal antibodies and the selection of variants with potential epidemiological significance. Virology 1980;104:139–48.
[24] Peng Y, Wang D, Wang J, Li K, Tan Z, Shu Y, et al. A universal computational model for predicting antigenic variants of influenza A virus based on conserved antigenic structures. Sci Rep. 2017;7:42051.
[25] Steinbruck L, Klingen TR, McHardy AC. Computational prediction of vaccine strains for human influenza A (H3N2) viruses. J Virol 2014;88:12123–32.
[26] Neher RA, Bedford T, Daniels RS, Russell CA, Shraiman BI. Prediction, dynamics, and visualization of antigenic phenotypes of seasonal influenza viruses. Proc Natl Acad Sci U S A. 2016;113:E1701–9.
[27] Klingen TR, Reimering S, Guzman CA, McHardy AC. In silico vaccine strain prediction for human influenza viruses. Trends Microbiol 2018;26:119–31.
[28] Steinbruck L, McHardy AC. Inference of genotype-phenotype relationships in the antigenic evolution of human influenza A (H3N2) viruses. PLoS Comput Biol 2012;8:e1002492.
[29] Smith DJ, Lapedes AS, de Jong JC, Bestebroer TM, Rimmelzwaan GF, Osterhaus AD, et al. Mapping the antigenic and genetic evolution of influenza virus. Science 2004;305:371–6.
[30] Koel BF, Burke DF, Bestebroer TM, van der Vliet S, Zondag GC, Vervaet G, et al. Substitutions near the receptor binding site determine major antigenic change during influenza virus evolution. Science 2013;342:976–9.
[31] Koel BF, Mogling R, Chutinimitkul S, Fraaij PL, Burke DF, van der Vliet S, et al. Identification of amino acid substitutions supporting antigenic change of influenza A(H1N1)pdm09 viruses. J Virol 2015;89:3763–75.
[32] Koel BF, van der Vliet S, Burke DF, Bestebroer TM, Bharoto EE, Yasa IW, et al. Antigenic variation of clade 2.1 H5N1 virus is determined by a few amino acid substitutions immediately adjacent to the receptor binding site. MBio. 2014; 5: e01070-14.
[33] Archetti I, Horsfall Jr FL. Persistent antigenic variation of influenza A viruses after incomplete neutralization in ovo with heterologous immune serum. J Exp Med. 1950;92:441–62.
[34] Smith DJ, Forrest S, Ackley DH, Perelson AS. Variable efficacy of repeated annual influenza vaccination. Proc Natl Acad Sci U S A. 1999;96:14001–6.
[35] Lee MS, Chen JS. Predicting antigenic variants of influenza A/H3N2 viruses. Emerg Infect Dis 2004;10:1385–90.
[36] Harvey WT, Benton DJ, Gregory V, Hall JP, Daniels RS, Bedford T, et al. Identification of Low- and High-Impact Hemagglutinin Amino Acid Substitutions That Drive Antigenic Drift of Influenza A(H1N1) Viruses. PLoS Pathog 2016;12:e1005526.
[37] Fonville JM, Wilks SH, James SL, Fox A, Ventresca M, Aban M, et al. Antibody landscapes after influenza virus infection or vaccination. Science 2014;346:996–1000.
[38] Anderson CS, McCall PR, Stern HA, Yang HM, Topham DJ. Antigenic cartography of H1N1 influenza viruses using sequence-based antigenic distance calculation. Bmc Bioinform 2018;19.
[39] Gupta V, Earl DJ, Deem MW. Quantifying influenza vaccine efficacy and antigenic distance. Vaccine 2006;24:3881–8.
[40] Bonomo ME, Deem MW. Predicting Influenza H3N2 Vaccine Efficacy from Evolution of the Dominant Epitope. Clinical infectious diseases: an official publication of the Infectious Diseases Society of America; 2018.
[41] Deem MW, Pan KY. The epitope regions of H1-subtype influenza A, with application to vaccine efficacy. Protein Eng Des Sel 2009;22:543–6.
[42] Li X, Deem MW. Influenza evolution and H3N2 vaccine effectiveness, with application to the 2014/2015 season. Protein Eng Des Sel 2016;29:309–15.
[43] Munoz ET, Deem MW. Epitope analysis for influenza vaccine design. Vaccine. 2005;23:1144–8.
[44] Pan K, Subieta KC, Deem MW. A novel sequence-based antigenic distance measure for H1N1, with application to vaccine effectiveness and the selection of vaccine strains. Protein Eng Des Sel. 2011;24:291–9.
[45] Sun H, Yang J, Zhang T, Long LP, Jia K, Yang G, et al. Using sequence data to infer the antigenicity of influenza virus. mBio 2013; 4.
[46] Skarlupka AL, Owino SO, Suzuki-Williams LP, Crevar CJ, Carter DM, Ross TM. Computationally optimized broadly reactive vaccine based upon swine H1N1 influenza hemagglutinin sequences protects against both swine and human isolated viruses. Hum Vaccin Immunother 2019;15:2013–29.
[47] Carter DM, Bloom CE, Nascimento EJ, Marques ET, Craigo JK, Cherry JL, et al. Sequential seasonal H1N1 influenza virus infections protect ferrets against novel 2009 H1N1 influenza virus. J Virol 2013;87:1400–10.
[48] Council NR. Guide for the care and use of laboratory animals, 8 ed. Washington, DC: The National Academies Press; 2011.
[49] Congress U. Transportation, sale, and handling of certain animals. In: Agriculture USDo, editor. United States Code. United States: USDA; 2015.
[50] Richmond J, McKinney R. Biosafety in microbiological and biomedical laboratories. 4 ed. Washington, D. C.: U.S. Government Printing Office; 1993.
[51] Carter DM, Darby CA, Johnson SK, Carlock MA, Kirchenbaum GA, Allen JD, et al. Elicitation of Protective Antibodies against a Broad Panel of H1N1 Viruses in Ferrets Preimmune to Historical H1N1 Influenza Viruses. J Virol 2017;91.
[52] Organization WH. Network WGIS. Manual for the Laboratory Diagnosis and Virological Surveillance of Influenza: World Health. Organization 2011.
[53] Carter DM, Darby CA, Lefoley BC, Crevar CJ, Alefantis T, Oomen R, et al. Design and characterization of a computationally optimized broadly reactive hemagglutinin vaccine for H1N1 influenza viruses. J Virol 2016;90:4720–34.
[54] Agency EM. Guideline on influenza vaccines: Non-clinical and clinical module [Draft]. In: Use CfMPfH, editor. EMA/CHMP/VWP/457259/2014. London E14 4HB , UK2014.
[55] Gaush CR, Smith TF. Replication and plaque assay of influenza virus in an established line of canine kidney cells. Appl Microbiol 1968;16:588–94.
[56] Winter G, Fields S, Brownlee GG. Nucleotide sequence of the haemagglutinin gene of a human influenza virus H1 subtype. Nature 1981;292:72–5.
[57] Nobusawa E, Aoyama T, Kato H, Suzuki Y, Tateno Y, Nakajima K. Comparison of complete amino-acid-sequences and receptor-binding properties among 13 serotypes of hemagglutinins of influenza a-viruses. Virology 1991;182:475–85.
[58] Burke DF, Smith DJ. A recommended numbering scheme for influenza A HA subtypes. PLoS ONE 2014;9:e112302.
[59] Wikramaratna PS, Rambaut A. Relationship between haemagglutination inhibition titre and immunity to influenza in ferrets. Vaccine. 2015;33:5380–5.
[60] RCoreTeam. R: A Language and Environment for Statistical Computing. In: Computing RFfS, editor. 3.6.2 ed. Vienna, Austria; 2013.
[61] Ghendon Y. The immune response to influenza vaccines. Acta Virol 1990;34:295–304.
[62] Monto AS, Petrie JG, Cross RT, Johnson E, Liu M, Zhong W, et al. Antibody to influenza virus neuraminidase: an independent correlate of protection. J Infect Dis 2015;212:1191–9.
[63] Angeletti D, Gibbs JS, Angel M, Kosik I, Hickman HD, Frank GM, et al. Defining B cell immunodominance to viruses. Nat Immunol 2017;18:456–63.
[64] Blackburne BP, Hay AJ, Goldstein RA. Changing selective pressure during antigenic changes in human influenza H3. PLoS Pathog 2008;4:e1000058.
[65] Schotsaert M, Ibanez LI, Fiers W, Saelens X. Controlling influenza by cytotoxic T-cells: calling for help from destroyers. J Biomed Biotechnol 2010;2010:863985.
[66] Rajao DS, Anderson TK, Kitikoon P, Stratton J, Lewis NS, Vincent AL. Antigenic and genetic evolution of contemporary swine H1 influenza viruses in the United States. Virology 2018;518:45–54.
[67] Anderson TK, Campbell BA, Nelson MI, Lewis NS, Janas-Martindale A, Killian ML, et al. Characterization of co-circulating swine influenza A viruses in North America and the identification of a novel H1 genetic clade with antigenic significance. Virus Res 2015;201:24–31.
[68] Liu STH, Behzadi MA, Sun W, Freyn AW, Liu WC, Broecker F, et al. Antigenic sites in influenza H1 hemagglutinin display species-specific immunodominance. J Clin Investig 2018;128:4992–6.
[69] Koedijk D, Pastrana FR, Hoekstra H, Berg SVD, Back JW, Kerstholt C, et al. Differential epitope recognition in the immunodominant staphylococcal antigen A of Staphylococcus aureus by mouse versus human IgG antibodies. Sci Rep 2017;7:8141.

[70] Vaughan K, Kim Y, Sette A. A comparison of epitope repertoires associated with myasthenia gravis in humans and nonhuman hosts. Autoimmune Dis 2012;2012:403915.
[71] Sutton TC, Chakraborty S, Mallajosyula VVA, Lamirande EW, Ganti K, Bock KW, et al. Protective efficacy of influenza group 2 hemagglutinin stem-fragment immunogen vaccines. npj Vaccines 2017;2:35.
[72] Lees WD, Moss DS, Shepherd AJ. A computational analysis of the antigenic properties of haemagglutinin in influenza A H3N2. Bioinformatics 2010;26:1403–8.
[73] Park AW, Daly JM, Lewis NS, Smith DJ, Wood JL, Grenfell BT. Quantifying the impact of immune escape on transmission dynamics of influenza. Science 2009;326:726–8.
[74] Wang P, Zhu W, Liao B, Cai L, Peng L, Yang J. Predicting Influenza Antigenicity by Matrix Completion With Antigen and Antiserum Similarity. Front Microbiol 2018;9:2500.
[75] Belshe RB, Gruber WC, Mendelman PM, Mehta HB, Mahmood K, Reisinger K, et al. Correlates of immune protection induced by live, attenuated, cold-adapted, trivalent, intranasal influenza virus vaccine. J Infect Dis 2000;181:1133–7.
[76] Lee MS, Mahmood K, Adhikary L, August MJ, Cordova J, Cho I, et al. Measuring antibody responses to a live attenuated influenza vaccine in children. Pediatr Infect Dis J 2004;23:852–6.
[77] Jurchott K, Schulz AR, Bozzetti C, Pohlmann D, Stervbo U, Warth S, et al. Highly Predictive Model for a Protective Immune Response to the A(H1N1)pdm2009 Influenza Strain after Seasonal Vaccination. PLoS ONE 2016;11:e0150812.